EVS26
Los Angeles, California, May 6-9, 2012

Adaptive Semi-Global Energy Management for a Series Hybrid Performance Vehicle – The Lotus 414E

Adam Chapman, Leon Rosario
Lotus Engineering, Potash Lane, Norfolk, NR14 8EZ United Kingdom
Email: achapman2@lotuscars.com

Abstract

The latest addition to Lotus Engineering's low carbon vehicle demonstrators is the Lotus Evora 414E. This series hybrid sports car is capable accelerating from 0-60mph in less than 4.5 seconds, yet produces less than 50g of CO2 per kilometre on the ECE-R101 emissions test. The vehicle showcases new developments in plug-in, range-extended electric propulsion, new electronic technologies to enhance driver involvement and torque vectoring. The vehicle is equipped with a 35kW normally aspirated Lotus range extender engine and a 300kW, 14kWh battery-pack to power the twin-motor driveline. To manage the system energy flow between battery, range-extender system and vehicle loads, an adaptive energy management technique has been developed. The energy management framework is capable of multi-objective optimisation over a variable time horizon. Arbitration of power flow is derived by evaluating the instantaneous cost functions for the battery and range extender respectively. The energy manager calculates the average vehicle power demand over a series of trailing time windows and evaluates instantaneous cost functions before determining the feed forward range extender operating point. Details of the energy management module developed for the Lotus 414E are presented in this paper. Implementation methods are discussed to demonstrate operation of the control system.

Keywords— Series Hybrid, Energy Management, Range Extender

1. Introduction

The Energy management strategy for Lotus' hybrid electric driveline is based on a transient fuel consumption model of the range extender engine and an equivalent fuel consumption model of the battery that incorporates a charge-sustaining strategy that considers the average efficiencies of the battery. Different from the instantaneous and global optimisation strategies, the optimisation problem is formulated over a relatively short time horizon characterised by the quasi-steady-state time constant of the Lotus Range Extender (LRE) engine. This is a Semi-Global Optimisation (SGO) strategy. To obtain a real-time implementable solution to this problem, a two-stage optimisation procedure is proposed. A preliminary solution is obtained from the Static Instantaneous Optimisation (SIO) and it is further adaptively filtered to optimise the RE operation using dynamic compensation optimisation. Simulation tests are presented to validate the proposed power and energy management strategy.

Figure 1: The Lotus 414E series hybrid high performance vehicle

2. Driveline Architecture

The series hybrid driveline comprises of the 35kW normally aspirated Lotus Range Extender (LRE) [1] engine coupled to a permanent magnet generator. The range extender engine, generator and generator inverter forms the Auxiliary Power Unit (APU). The

battery pack comprises of 1,792 Lithium Iron Phosphate (LiFePo) cells configure.d as a 112 Series-16 Parallel pack. Propulsion is provided by two independently driven rear wheel motors. For plug-in functionality, the vehicle is equipped with a 3kW onboard charger. Representation of the vehicle driveline is shown in Fig. 2.

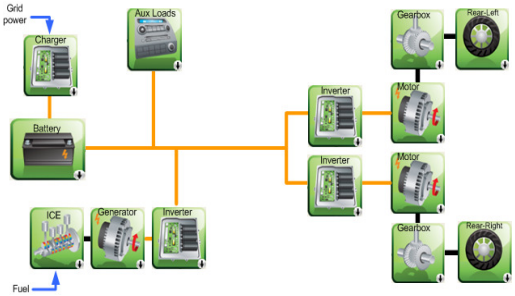

Figure 2. Lotus 414E Driveline Architecture

There are two states where the battery energy may be replenished. The condition where energy is returned to the battery via the range extender engine or via the on-board charger is termed a "recharging". The state where energy is returned to the battery through regenerative braking is termed as "recovering". Both conditions may exist simultaneously where the energy returning to the battery is the algebraic sum of the powers from APU charging and kinetic energy recovery.

The battery assumes the operation of a bidirectional electrical power system while the APU assumes operation of a unidirectional power delivery system. Power flow control is achieved by regulating the voltage and currents of the generator inverter as well as engine speed and torque. The power flow convention is illustrated in Fig. 3. Bidirectional arrows indicate bidirectional power and current flow.

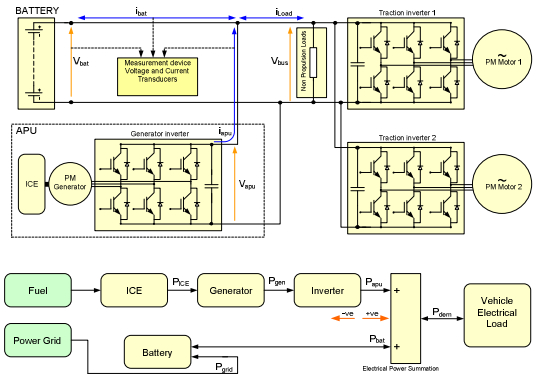

Figure 3. Lotus 414E Driveline Schematic and Power Flow Convention

3. Energy Management System (EMS)

This section describes the formulation of the battery and APU cost functions and the evaluation method used to determine the feed forward operating point of the APU.

3.1 Semi-Global Optimisation

The online optimisation of driveline efficiency is based on the battery-equivalent cost function approach from [2]. The EMS is tasked not only to control the delivery of power to the vehicle's propulsion load, but also the auxiliary electrical loads in the most efficient manner possible. The total electrical power demand is measured on the DC bus and recorded at a minimum sampling frequency, determined in simulation, to be 10Hz.

A cost function is introduced which defines the fuel equivalent cost of energy delivered by both the battery and the APU, in units of grams per Joule. The cost function format is defined as

$$J_t(P_{apu}, \dot{P}_{apu}, \mathrm{SoC}) = C_{apu}(P_{apu}, \dot{P}_{apu}) + C_{bat}(P_{bat}, \mathrm{SoC}), \quad (1)$$

where J_t is the fuel-equivalent cost at time t,

P_{apu} is the vehicle's electrical power consumption,

$\dot{P}_{apu}$ is the rate of change in vehicle electrical power,

SoC is the battery State of Charge at time t,

C_{apu} is the fuel cost of APU energy,

C_{bat} is the fuel cost of battery energy,

P_{bat} is the battery power.

A global optimisation would optimise over an entire drive cycle, and would need knowledge of the drive cycle a priori. In the real world, it is impractical to precisely predict the power demand profile of a vehicle throughout its journey. Instead the method presented here aims for a semi-global optimisation, analysing the most recent power demands of the vehicle and calculating a minimum cost for the near future power demand over a very small future time horizon. If the sampling rate is 10 Hz, the future time horizon that the method applies optimisation to is only 0.1 seconds.

We calculate the average vehicle power demand over a series of trailing time windows, of size 1-20 seconds, in one second steps [2]. When the vehicle power demand is oscillatory about a single load point, the optimiser calculates that it is more efficient to deliver the mean APU power

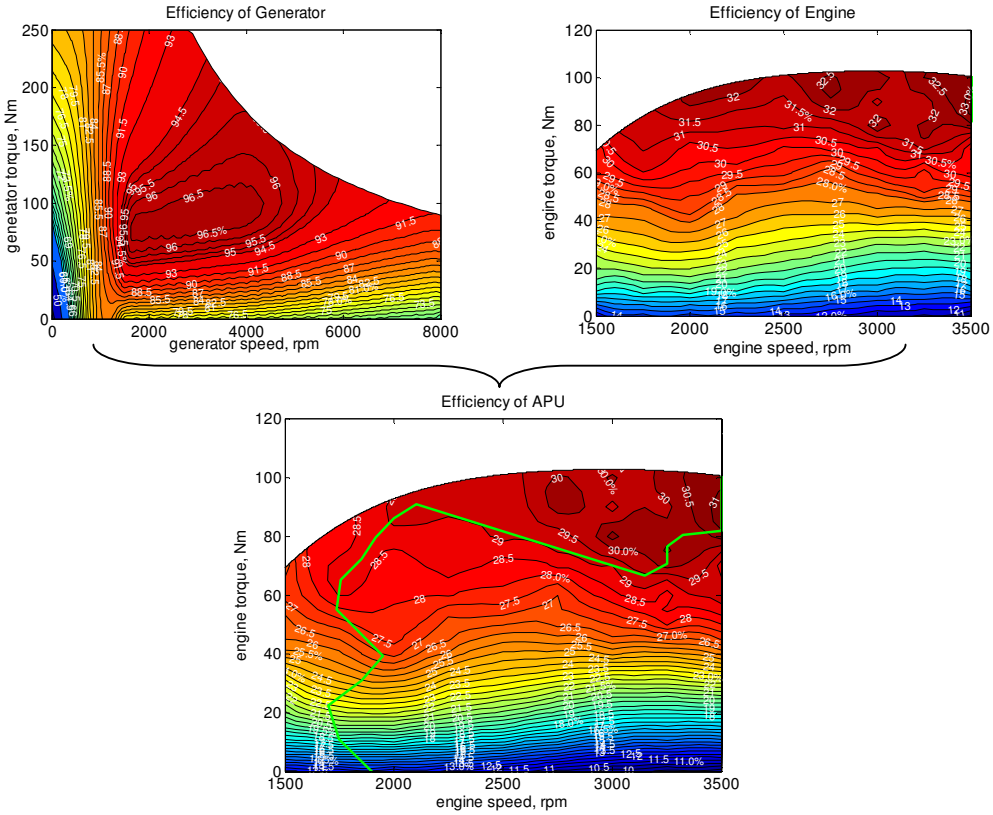

Figure 4. APU efficiency with Q_f = 43x10^6 J/kg. Green line shows optimal APU operation locus

demand over the cycle than to instantaneously match the power demand of the vehicle as it oscillates. The fuel equivalent cost, Jt is calculated by the EMS at each 0.1 second time step. It is evaluated for each of the moving average power demands, substituting Papu with the moving average power demands. The resulting Papu which corresponds to the minimum instantaneous cost is demanded from the APU by the EMS. In the following discussion the individual constituents of the EMS are defined and explained, with reasoning for their inclusion to the system.

3.2 APU Power Cost Function

It is ideal for the APU to deliver electrical energy at maximum fuel efficiency; hence a locus of minimal fuel consumption per unit energy, for individual power demands, was derived by combining the efficiency map of the generator and the BSFC map of the engine. Fig. 4 shows the resulting APU efficiency map, assuming the calorific value of fuel is 43x106 J/kg.

The fuel-equivalent cost of the APU power is calculated from the efficiency map in Fig. 4 and the calorific value of the fuel. A transient correction factor is included to account for extra fuel consumption during transient power demands [3]. The APU fuel cost can be expressed as,

$$C_{\text{apu}} = \left(\frac{P_{\text{apu}} \eta_{\text{inv}}}{Q_f \eta_{\text{apu}}} \right) \times \left(1 + k \left| \dot{P}_{\text{apu}} \right| \right) \qquad (2)$$

where Q_f is the fuel's calorific value in J/kg,

η_{apu} is the APU efficiency on the optimal locus for power (as per Fig. 4),

k is a transient correction coefficient (7% per 10kW/s),

η_{inv} is the inverter efficiency, assumed to be 95% in simulation.

We use a 7% increase in fuel consumption for a power gradient of 10 kW/s for k. This is the value used in [3] and correlates well with the Lotus Range Extender engine. In the future it would be useful to study the most efficient speed-torque route between two optimal power coordinates, in respect to the amount of extra fuel used in transient states. An experimental procedure similar to the one described in [3] would need to be employed, with variations in both speed and torque.

3.3 Battery Power Cost Function

In [2] an attempt is made to calculate the round-trip efficiency of energy passing in and out of the battery by projecting an assumed mean discharge efficiency and applying it in the calculation of fuel-equivalent charge cost. Instead of applying a fixed efficiency supposition at all times, we accumulate average charge and discharge efficiencies over time, starting from the moment the charge-sustaining operation mode is initiated.

Battery efficiency is calculated using steady-state I^2R loss and open-circuit voltage:

$$\eta_{\text{bat}} = \frac{IV_{\text{oc}} - I^2R}{IV_{\text{oc}}} \tag{3}$$

If transient voltage characteristics are included, equation (3) becomes

$$\eta_{\text{bat}} = \frac{IV_{\text{oc}} - I^2R - IV_{\text{trans}}}{IV_{\text{oc}}} \tag{4}$$

where V_{trans} is the voltage correction due to transient effects. Attempts were made in this study to determine dynamic battery characteristics. The approximate battery dynamic characteristics derived where used in the simulation model of the battery, but deemed not reliable enough to use in the knowledge based look-forward controller.

In the look-ahead battery model used in the EMS, the instantaneous battery efficiency corresponding to a given battery discharge power is

$$\eta_{dis} = \left(\frac{1}{2} + \frac{1}{2}\sqrt{1 - \frac{4R_{\text{dis}}\left|P_{\text{bat}}\right|}{V_{\text{oc}}}} \right) \tag{5}$$

and battery efficiency during a charging instant is

$$\eta_{\text{chg}} = \left(\frac{1}{2} + \frac{1}{2}\sqrt{1 - \frac{4R_{\text{chg}}\left|P_{\text{bat}}\right|}{V_{\text{oc}}}} \right). \tag{6}$$

R_{dis} and V_{oc} are evaluated from lookup tables with respect to the SoC of the battery.

3.3.1 Charge Cost

An attempt to calculate the round-trip energy fuel equivalent cost is made by projecting the mean discharge efficiency onto the future vehicle power demands. Hence the instantaneous fuel-equivalent battery charge cost is determined using

$$C_{\text{bat,chg}}\left(P_{\text{bat}}, SoC\right) = \frac{P_{\text{bat}}\overline{C}_{\text{apu}}}{\overline{\eta}_{\text{dis}}\eta_{\text{chg}}\overline{P}_{\text{apu}}} \tag{7}$$

where $\overline{C}_{\text{apu}}$ is the mean APU cost, measured in grams per second and, like all mean parameters denoted by the bar notation, is calculated inside the EMS using a trapezium rule for approximate integration. Initiating at zero on every trip allows the EMS to quickly accumulate an average value that is specific to trip-specific driving behaviour.

3.3.2 Discharge Cost

The fuel-equivalent cost of a discharging power drawn from the primary battery is calculated by

$$C_{\text{bat,dis}}\left(P_{\text{bat}}, SoC\right) = \frac{\delta\, P_{\text{bat}}\overline{C}_{\text{chg}}}{\overline{\eta}_{\text{chg}}\eta_{\text{dis}}P_{\text{apu}}}, \tag{8}$$

The average charge cost, $\overline{C}_{\text{chg}}$, is used to quantify the mean amount of fuel associated with each unit of energy in the battery at the current point in time. η_{dis} is the instantaneous battery discharge efficiency.

It is important to note that discharge cost is more accurate than the charge cost calculation, because there is no requirement to "look ahead" in order to calculate a round-trip energy path efficiency and equivalent fuel cost.

The term δ, introduced from [4], is used to describe the ratio of total energy in the battery at any time that is the result of combusting fuel in the APU. When the APU charges the battery, δ increases. During a regenerative braking event, δ decreases, and as a result the fuel-equivalent cost of battery discharge power is reduced. It is determined using

$$\delta = \frac{\int P_{\text{bat,apu}}\, dt}{\int \left(P_{\text{bat,apu}} + P_{\text{bat,non-apu}}\right) dt}. \tag{9}$$

Cautious calculation is required during periods of battery discharging, as the fraction δ remains constant while the denominator term reduces. When the battery is replenished with a plug-in charge, δ reduces as the non-APU energy in the denominator increases and the numerator term remains constant.

3.4 Cost Function Evaluation

As per equation (1), the combined cost function for APU and battery operation in charge-sustaining mode defined by

$$J_t(P_{apu}, \dot{P}_{apu}, \text{SoC}) = C_{apu}(P_{apu}, \dot{P}_{apu}) + C_{bat}(P_{bat}, \text{SoC}) \quad (10)$$

Instead of instantaneously matching the APU power demand with the APU, the EMS tracks moving averages of vehicle power demand varying from 0 seconds to 20 seconds. The total demand P_{dem} is simply the sum of P_{apu} and $P_{bat.}$ When the battery reaches a lower SoC boundary of 40% (All Electric Range), charge-sustaining operation is initiated. At the start of charge-sustaining mode, P_{dem} is set $P_{bat.}$ This is done as there is no historical APU power demand at the start of the charge sustaining mode.

At 0.1 second internals, the EMS evaluates P_{dem}, accumulates a 0-20 second moving averages and then calculate the fuel-equivalent cost of providing APU power equal to each of those moving average values. The zero second moving average is effectively the instantaneous power demand, which allows the APU to adopt a load-following strategy if the associated cost function determines it to be optimal. The moving average power demands are applied to the cost function as "trial values" of APU power demand, P_{apu} in (1). The battery power, P_{bat} is then evaluated as the difference between demand and APU power,

$$P_{bat} = P_{dem} - P_{apu} \quad (11)$$

Of all the moving average powers analysed, the one which corresponds to the minimum fuel-equivalent cost is requested by the EMS to the APU. The APU power demand is then expressed as

$$P_{\text{APUdemand}} = \min_{\text{t=movavg}} J_t \quad (12)$$

i.e. the trial power demand corresponding to the moving average period for which fuel-equivalent cost is minimal.

A 3-second moving average is applied to the APU power demand evaluated in (12) to remove any fast oscillatory behaviour of the APU. Operation of the EMS is summarized as a flowchart in Fig. 5.

3.5 Additional control laws

Extra features have been added to the original cost functions which function to protect the vehicle hardware (particularly batteries) from exceeding their physical limits.

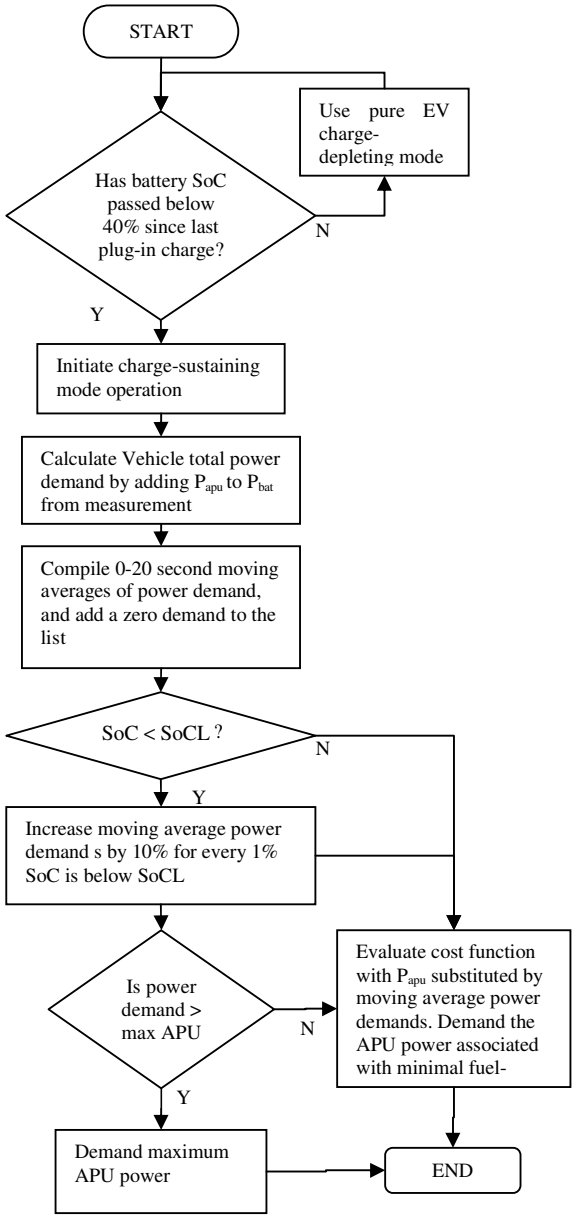

Figure 5. Flowchart of the EMS, repeated in the vehicle controller at every time step.

3.5.1 Protection from SoC depleting in charge-sustain mode

The traction motors on the 414E vehicle are capable of consuming more power than the APU can provide. In order to stabilise the battery SoC during and after high traction power demand periods, we introduce two new control rules:

1. When traction power demand is more than or equal to the maximum APU power, ignore the cost of moving average power demands and run the APU at maximum power.

2. We implement an advisory lower state-of-charge limit, $SoCL$. When $SoC < SoCL$, the instantaneous power demand fed into the optimisation algorithm is multiplied by a factor by γ. In experimental testing, it was found that increasing the perceived power demand by 10% for every 1% that SoC is below $SoCL$ was sufficient.

These two new rules limit the depletion of battery charge during high tractive power demand periods and aid recovery back towards $SoCL$ after a high power demand event.

3.5.2 Kinetic energy compensation

The lower state of charge recommendation $SoCL$, is reduced in real time in accordance with the forward velocity of the vehicle. This is because the battery will regain approximately the same amount of energy when it decelerates to rest, minus the energy spent on aerodynamic drag and rolling resistances [5], as well as powertrain efficiencies.

3.5.2 Battery Voltage Protection

If at any of the moving average power demands considered by the EMS are smaller than the vehicle power demand measured on the DC bus to such an extent that the battery voltage would drop below a defined limit (2.1 volts per cell), the cost of those APU power options are set to infinity. This effectively prevents the APU from running at a power output too low for the battery voltage to be maintained at or above the minimum absolute limit.

4. Calculating Vehicle Power Demand

The vehicle power is measured by summation of the battery and APU powers. Battery voltage and current values are measured within the battery pack and is available over CAN. The APU power is calculated by multiplying the APU current by the DC bus voltage as shown in Fig. 6.

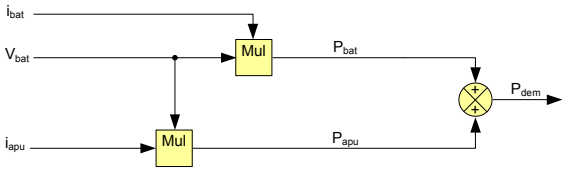

Figure 6. Measurement of vehicle power demand Pdem.

5. Simulation Results

The all electric range is calculated by repeating a specified drivecycle in simulation until the battery depletes from 100% to 40% SoC. Charge sustaining range simulations begin with battery SoC at 40% and run until the entire tank capacity (30 litres) of fuel has been used, after which the simulated distance covered is recorded. A trace of SoC and APU power is shown over four consecutive NEDC cycles in Fig. 7.

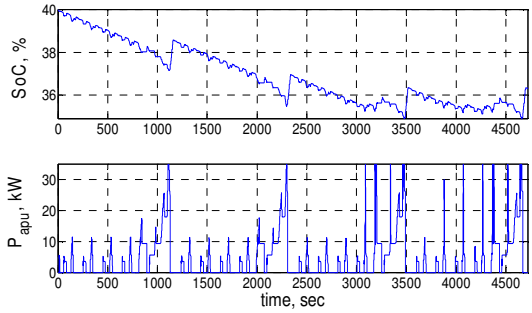

Figure 7. Battery SoC and APU power over repeated NEDC cycles. SoC drops in the 1st 3 cycles as mean APU cost is accumulated

The weighted CO_2 in grams per km, M, is calculated as

$$M = \frac{25M_{cs}}{D_e + 25}, \tag{13}$$

where D_e is the electric-only range of the vehicle and M_{cs} is the mass of CO_2 emitted from the tailpipe during one drive cycle in charge-sustain mode operation. This convention is defined for the NEDC cycle but a similar calculation has been performed using data recorder on the Combined Artemis cycle, which is considered to closely represent real-world driving behaviour [6]. The vehicle's electric range was calculated to be 52.6 km on the NEDC drivecycle and 46.2 km on the combined Artemis cycle. Performance simulation results are shown in Table 1, with the un-weighted CO_2 figure being measured over a full-tank depletion simulation, equivalent to about 500 km of driving in charge-sustaining mode.

Table 1. Weighted and un-weighted CO_2 from simulation

NEDC	Weighted CO_2 (g/km)	Un-weighted CO_2 (g/km)
Adaptive EMS	38.5	132
Load Following	51.1	159
Stop-start	38.4	128
ARTEMIS	**Weighted CO_2 (g/km)**	**Un-weighted CO_2 (g/km)**
Adaptive EMS	52.9	160
Load Following	57.6	165
Stop-start	54.6	155

Table 1 also shows comparison Figures of the Adaptive EMS proposed in this paper with load-following strategy and a simple stop-start (thermostatic) strategy.

With the load-following method, the APU provides the instantaneous power demand, P_{dem} with APU power being limited between 3 kW and 35 kW. When the battery SoC drops below 35%, the APU provides 35 kW until SoC is equal to 40%.

In the implementation of the stop-start strategy, the APU only runs at 35 kW, which is the power at which the engine BSFC is optimal. The battery cycles between 35% and 40% SoC, with the APU delivering a continuous 35kW when SoC drops below 35% SoC and 0kW when SoC is equal to 40% SoC. It is important to note that this simple start-stop method does not assume any battery charging power constraints and can only be implemented if the battery pack is receptive to high charging rates.

The simulation results in Table 1 shows that the stop-start strategy produces less un-weighted CO_2 emissions. The simulation data in Fig. 8 also shows that the CO_2 emitted using start-stop drops below the CO_2 of the proposed adaptive EMS as the charge sustaining range increases on the Artemis cycle. This is because in the start-stop method, the APU runs, on average, at a higher efficiency load-point than the proposed adaptive EMS. This is only true because the battery on the 414E is receptive to continuous high power charging (35kW). The fact that the emitted CO_2 figures of the proposed EMS (which considers battery constraints) is very close to start-stop method shows that adaptive nature of the proposed controller.

5.1 Adaptive nature of the EMS

Although developed for a high-performance vehicle, the adaptive nature of the EMS lends itself beneficial to any series hybrid platform. The following demonstrates the effectiveness of the EMS based on

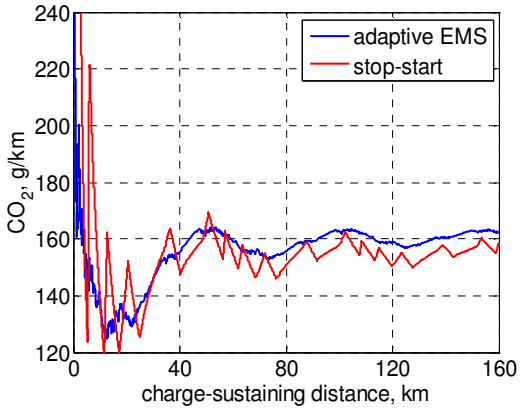

Figure 8. Comparison of M_{cs} between adaptive EMS and stop-start method on repeated Artemis cycles

a statistical usage patterns of vehicles. Recording the probability of the adaptive EMS producing fewer emissions than the stop-start strategy with distance, from Fig. 8, we employ Bayes' theorem to infer a probability that the proposed EMS performs favourably for charge-sustaining operation on an arbitrary trip. To demonstrate this, daily driving distance data from [7], recorded over 179,484 separate daily journeys, was used. Subtracting the Artemis-cycle electric range of 46.2 km leaves the normalised probability distribution of distances travelled in charge-sustaining operation shown in Fig. 9.

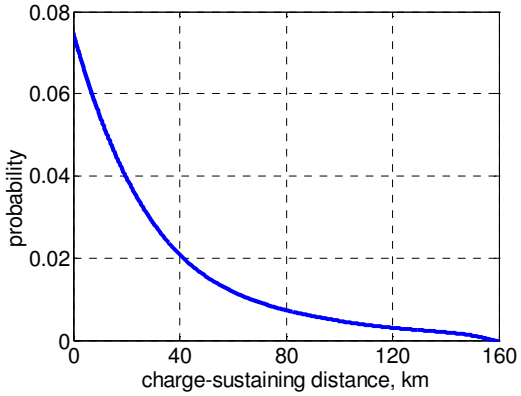

Figure 9. Probability distribution of charge-sustaining trip distances

Using Bayes' theorem, the probability of a the adaptive EMS consuming less fuel than a stop-start strategy and hence producing fewer CO_2 emissions, given that the probability of charge-sustaining distance covered is similar to that in Fig. 9, is 98.8%.

6. Future Work

The cost function is not restricted to seeking an optimal value of a single variable. A multi-objective approach, as attempted in [8] uses a weighted sum of separate cost functions for specific targets, e.g. fuel consumption, battery life and emissions. The weighting factors do not need to be fixed, and can be altered during the lifetime of the vehicle in order to concur with future emissions standards. The weighting factors could even be modified in accordance with local emissions restrictions during a journey.

By employing *moving* averages of mean APU and battery charge/discharge cost as opposed to the constant assumed values [2,4], the proposed EMS will be able to adapt to driver behaviour over a short trailing time window. For example, if the vehicle exits a motorway and continues to drive along country roads, the average APU power will drop significantly and a moving average value of APU cost will quickly adapt to local driving conditions.

7. Conclusions

The adaptive Energy Management System for the Lotus 414E Series Hybrid vehicle platform has been presented. A mathematical framework has been described that is able to optimise fuel consumption in charge-sustaining mode on a series hybrid vehicle, with consideration of physical system limitations and protective measures to prevent degradation of system components. The framework is extendable by adding additional objectives to the cost function. Simulation results demonstrate the effectiveness of the EMS on the Lotus 414E and series-hybrid vehicles in general. The EMS has been implemented within the Lotus Vehicle Controller hardware and is undergoing verification tests.

8. References

[1] Turner J., Blake D., Moore J., Burke P., Pearson R., Patel R., Blundell D., Chandrashekar R., Matteucci L., Barker, P. and Card, C. "The Lotus Range Extender Engine for Plug-In Series Hybrid Vehicles" *SAE 2010 Powertrains, Fuels & Lubricants Meeting*

[2] He, B. and M. Yang. "Optimization-based energy management of series hybrid vehicles considering transient behaviour." *International Journal of Alternative Propulsion* ***1****(1): 79-96., 2006*

[3] Pelkmans, L., Coenen, P. and Vermeulen, F. (1998) "Estimation of the real-world emissions of a series hybrid vehicle". *Proceedings of the 15th International Electric Vehicle Symposium.*

[4] Liangfei Xu, Guijun Cao, Jianqiu Li, Fuyuan Yang, Languang Lu and Minggao Ouyang (2010). "Equivalent Consumption Minimization Strategies of Series Hybrid City Buses" *State Key Lab of Automotive Safety and Energy, Tsinghua University, P.R.China, 2010*

[5] Chapman, A. and Pearson, R. "An assessment of the energy efficiency and emissions outputs of electric and hybrid-electric vehicles", *Les Rencontres Scientiques d'IFP Energies nouvelles Int. Scient. Conf. on hybrid and electric vehicles - RHEVE 2011*

[6] Bassett, M., Fraser, N., Brooks, T., Taylor, G., Hall, J. and Thatcher, I., "A study of Fuel Converter Requirements for an Extended-Range Electric Vehicle", *SAE 2010 World Congress & Exhibition, April 2010*

[7] van Haaren, R. "Assessment of Electric Cars Range Requirements and Usage Patterns based on Driving Behavior recorded in the National Household Travel Survey of 2009". *Columbia University, December 2011*

[8] L. Serrao, A. Sciarretta, O. Grondin, A. Chasse, Y. Cre, D. di Domenico, P. Pognant-Gros, C. Querel, and L. Thibault. "Open Issues in Supervisory Control of Hybrid Electric Vehicles: A Unified Approach using Optimal Control Methods", *Les Rencontres Scientiques d'IFP Energies nouvelles Int. Scient. Conf. on hybrid and electric vehicles - RHEVE 2011*

Authors

Adam Chapman gained his MEng degree in Avionics & Aerospace Systems Engineering from the University of Manchester in 2008. He is currently Lotus' lead simulation developer and is working on optimal control of hybrid vehicles. His research interests include machine learning and model based control systems.

Leon Rosario gained his Ph.D. in Electrical and Electronics Engineering from Cranfield University in 2007. He is currently Executive Engineer with Lotus' hybrid and electric vehicle integration group. His research interests include power electronics, energy management and control theory.